CEST 2023

18th International Conference on Environmental Science and Technology

Athens, Greece, 30 August to 2 September 2023

Valorization of waste graphite deriving from "End of Life Lithium-Ion Battery recycling" for a second use in wastewater treatment.

PREMATHILAKE D.S.[1,*], BOTELHO JUNIOR A.B.[2], COLOMBI F.[1], TENORIO J.[2], ESPINOSA D.[2], VACCARI M..[1,*]

[1] CeTAmb Research Center, DICATAM, Università Degli Studi di Brescia, Italy (IT).

[2] LAREX, Department of Chemical Engineering, University of Sao Paulo, Brazil (BR).

*corresponding author:

e-mail: d.prematHilake@unibs.it, mentore.vaccari@unibs.it

Abstract: Exponential utilization of Lithium-ion batteries (LIBs) has produced a notable amount of hazardous waste recently. The current practices focus on recovering precious metals available in cathode giving less priority for anode material (graphite) recoveries and valorizations. However, thinning of existing graphite ores, and extensive application of graphite for high tech industries made graphite to be a critical raw material to Europe recently. Accordingly, an attempt was made to valorize black mass, after leaching of metals. The batteries were physically processed, and the product was leached using 1mol/L, H_2SO_4 at 90°C for 90min with solid-liquid ratio 1/10. The remaining material was rich in graphite, which was used in this study. Three adsorption materials; Graphite Oxide (GO), Graphene Oxide (GrO) and Exfoliated graphite (EG) were made from the black mass to be used in organically contaminated wastewater treatment. After physical and chemical characterization, batch adsorption experiments were carried out separately for three different spiked organic contaminated (MO, MG, and MB) wastewater samples. Adsorption kinetics and isotherms were determined to conclude the best valorization option for the spent graphite available in black mass of LIBs. Accordingly, the study concluded that GrO to be the best option for spent graphite valorization.

Keywords: LIB recycling, Graphite valorization, adsorption experiments, Wastewater treatment, Black mass recycling

1. Introduction

Current literature claimed that by the end of 2030, there would be 1 million spent LIBs and further it would reach up to 1.9 million by the end of 2040. Along with the higher accumulation of discarded LIBs and limited concerns on recycling of the same, several environmental and human safety threats are piling up. In fact, the threats are due to the hazardous nature of the waste LIBs, if contaminated with natural soil or water without proper recycling steps. Consequently, establishing sustainable procedures to recycle and reuse elements from spent LIBs will reduce the threats imposed to nature and the human safety and at the same time it will provide solutions to raw materials depletion from natural ores (Prematthilake et al., 2023).

The cathode of LIB mainly consists of transitional metal oxides attached to the aluminum foil as a thin layer mixed with organic binders. In contrast anode mainly contains graphite, or a similar graphitic material attached to copper foil as a thin material again mixed with organic binders. Graphite/ graphitic materials have several qualities to be selected as the anode material in the LIBs widely. Mainly, graphite has low working potential at ~0.15 V vs. Li+/Li and high theoretical capacity at around 372 mAh/g. Further, graphite is a stable material under range of temperature, and it is relatively cheaper than most of other competitive materials (Lahiri & Choi, 2013).

Among many other methods used for recovering precious materials from the waste LIBs, hydrometallurgy is the most favored. This is due to the mild state, low greenhouse gas emissions, and low energy requirement plus high recovery rates of valuable metals. Currently, priorities are given for cathode material recoveries which has a greater portion of material cost from the total battery associated with supply criticality. In contrast, anode parts which contain mostly graphite are filtered and discarded as per their lower economic value. However, compared to the recent enhanced usage of LIBs, the amount of discarded graphite would be significantly high given that each LIB contains 12-21 wt% of graphite (Maroufi et al., 2020). The waste graphite derived from LIBs contains hazardous contaminants (e.g., organic compounds) which are responsible for environmental degradation and human sanitation threats upon dispose to the environment. On the other hand, graphite has been identified as a strategic and critical material recently and extraction of the same has prohibited in many countries in America and Europe. Accordingly in near future, the price of the graphite willraise, and further substitutes or potential new sources are needed to be identified. Hence, in this study, we propose a novel approach to valorize and reuse waste graphite derived after recovery of cathodic metals in a different application to give it a second life.

2. Methodology

Twenty NMC 811 cylindrical batteries were completely discharged using Cu and Ni-Cr (4 Ohm) wire. Then a knife mill was used to physically process the batteries under 9.4 mm particles. After removing the plastics, separators, and electrolytes (through drying for 24 hours at 25 ^{0}C under the fume hood) the remaining materials were milled again to achieve particles below 2 mm for leaching. The leaching of cathodic metals was carried out using 1mol/L, H_2SO_4 for 90 min at 90^{0}C (optimized values) (Guimarães et al., 2022). The remaining material (waste graphite (WG)) after leaching was filtered, washed with deionized water, and dried for 24 hours at 60^{0}C to be taken for the next steps.

Preparation of adsorption materials

To prepare graphite oxide (GO) and graphene oxide (GrO) as adsorption materials, the Hummer's method was used (S. Hummers Jr. & E. Offeman, 2002). In preparation of GO, 10 g of WG was mixed with 230 mL of 98% H_2SO_4 at 5^{0}C and stirred at 180 rpm for 1 hour. After, 30g of 99% $KMnO_4$ was added to the mixture slowly, while stirring to avoid sudden temperature rises. Temperature was maintained under 40^{0}C while adding $KMnO_4$. The mixture was kept for additional 3 hours while stirring. At the end of the 3 hours, 460 mL of de-ionized water was added to the mixture using dropping funnel method to avoid rapid temperature rises. The temperature was increased gradually up to 90^{0}C by controlling the rate of de-ionized water addition. The mixture was stirred for 30 minutes more at90^{0}C. Then, 230 mL of deionized water was added using the dropping funnel method. Finally, 10 mL of 30%, H_2O_2 was added to the mixture and stirred for 15 minutes to stop the oxidation reaction.

Then, the mixture was filtered using a filter paper and the residue was washed with 3000 mL of 10% HCl for washing. Later, the residue was further cleaned using 1000 mL of 99% ethanol. After the filtration, the residue was further washed several times using excess amount of de-ionized water until the pH of the filtrate reaches a near neutral value (pH 5.5). Then, the residue was dried at 50^{0}C for 24 hours in the furnace and then grounded using pestle and mortar.

GrO was prepared by exfoliating a fraction of the prepared GO through ultrasonication (Ogino et al., 2014). 30 mg of prepared GO was charged to a propylene tube (30 mm outside Diameter and 115 mm length) with 15 mL of deionized water (S/L= 2 g/L). The mixture was sonicated (Ultrasonic Bath, Solid Steel, 100W) for 30 minutes (5 min *6). After every 5 minutes of sonication, the mixture was centrifuged at 3000 rpm for 5 minutes. At the end of the 30 minutes sonication, the mixture was filtered using a filter paper and dried at 50^{0}C for 24 hours in the furnace and then grounded using pestle and mortar.

Exfoliated Graphite (EG) was prepared by mixing 6 mL of 60% $HClO_4$, 5 g of WG and 5 g of Cu $(NO_3)_2$ (weight ratio 2:1:1) at room temperature under the fume hood. After, the mixture was uniformly distributed on a quartz beaker and operated in a domestic microwave oven at 800 W for 40 seconds (Saikam et al., 2022). The resulting material was kept under the fume hood until it completely cools down and then, dried at 50^{0}C for 24 hours in the furnace and then grounded using the pestle and the mortar.

Characterization of materials

WG derived after the recovery of precious metals from EoL LIBs was characterized by XRF-EDX (EDX-7000, Shimadzu), XRD (Miniflex, Rigaku), Particle size (Mastersizer 2000, Malvern), Carbon content (Elementrac CS, ELTRA GmbH) Raman Spectroscopy (InVia R.M., Renishaw) and SEM (Phenom ProX, Thermo Fisher). Adsorption materials made during the previous steps were characterized by XRD, SEM and Raman Spectroscopy.

Batch adsorption tests

The adsorption tests were carried out on a magnetic stirrer setup at 300 rpm speed. Methyl orange (MO), malachite green (MG) and methylene blue (MB) dyes were used as organic pollutants and their initial concentration in aqueous samples used in adsorption tests was set to 30 mg/L. 10 mg of each adsorbent materials (GO, GrO and EG) were added to 50 ml of stirring dye samples separately at room temperature (25^{0}C). The removal of dyes under aqueous solutions was studied at different time intervals (2-10 min).. 6 replications with varying dosages of adsorption materials (0.01-0.06 g) for each absorption test were undertaken to improve the reliability of the experiment.

Adsorption percentage of each dye by the adsorption materials was calculated using,

$$\boldsymbol{Adsorption}\ \% = \frac{C_0 - C_e}{C_0} \times 100\% \qquad (1)$$

And adsorption capacity of the dye by the adsorbent at equilibrium q_e (mg/g) was calculated using,

$$q_e = (C_0 - C_e) \times \frac{V}{m} \qquad (2)$$

Where, C_o and C_e are the concentration of the dye in liquid phase at initially and at equilibrium respectively in mg/L. V is the volume of the solution in L and m is the mass of the adsorbent in g.

3. Results and discussions

XRD analysis of WG showed that the sample contains graphite and metallic compounds derived from the LIB cathode (Figure 1). Hence, further analysis was taken into consideration to identify all the materials present in WG samples. Accordingly, Carbon content analyzer showed that the sample contains 96.57% carbon with particle sizes vary from 0.955 µm to 69.183 µm. XRF-EDX results suggested that other materials present in the samples are Cl (1.09%), Ni (1.05%), Co (0.38%), Al (0.38%), Mn (0.32%), Fe (0.05%) and other metals below 0.05%.

Raman spectra (Figure 2) of the WG confirmed that the graphite recovered is in "cleaved graphite" form (T.

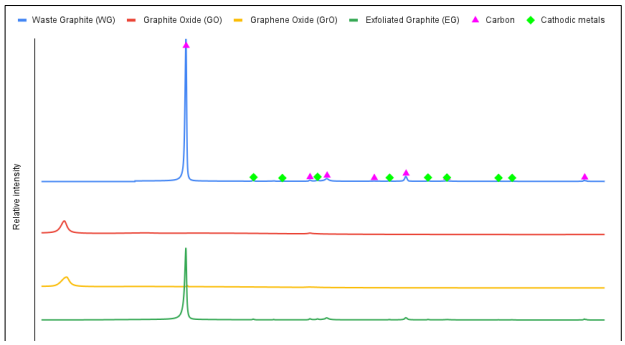

Figure 1: XRD patterns of WG, GO, GrO and EG

Tanabe et al., 1992).
SEM images (Figure 3.a) of the WG confirms that the morphology of the graphite is not significantly changed during the cycling and recovering processes. Though, the surface is not very smooth and subjected to minor deterioration. However, several impurities (mainly O –

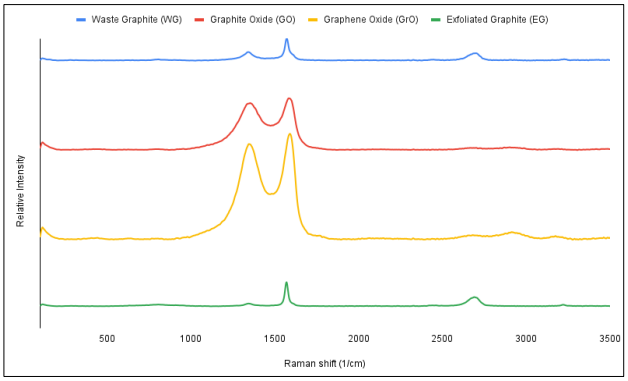

Figure 2: Raman Spectra of WG, GO, GrO and EG

around 10% and miner amounts of Al, Cl and S) and agglomerations are present in the samples analyzed. Further, SEI layer is not to be seen on the surface confirming that leaching has effectively removed it.

XRD, patterns of the materials show the correct formation of GO and EG when compared to the existing literature (Hidayah et al., 2017)(Saikam et al., 2022). XRD pattern of GrO is not fully understood in the current literature hence, formation of the same is hard to determine through XRD analysis.

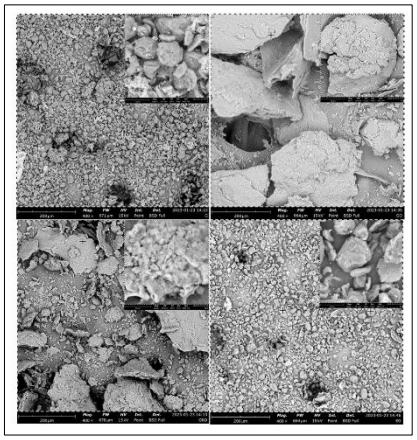

Figure 3: SEM images of a) WG, b) GO, c) GrO and d) EG

However, Raman spectra seems to be a better analysis to identify the formation of GrO. Accordingly, the Raman spectra pattern of the produced material matches with the commonly available graphene oxide's Raman spectra pattern. Moreover, Raman spectra of GO and EG further confirms the availability of those materials in the outcomes (Dhakate et al., 2011). SEM images of EG (Figure 3.d) is not formed its identical worm like structure (Saikam et al., 2022). The morphology of EG, is more like purified graphite recovered from EoL LIBs identified by (Ma et al., 2019). GO and GrO show a higher degree of oxidation and the C:O ratio has increased dramatically during the production as suggested by the SEM images. This implies the availability of a higher number of surface-active groups that can effectively adsorb substances.

In adsorption experiments of dyes, the effect of time on MB removal was determined for each of the adsorbent materials modified. Accordingly, GO removed MB at 98% efficiency, GrO removed MB at 90% efficiency and EG removed MB at 6.5% efficiency at the end of 10 min. After, the effect of time was studied only for GO for each dye. The results are shown in Table 1.

Table 1: Removal Efficiency (%) of all dye types by GO and GrO adsorption materials after 10 min.

	MB	**MG**	**MO**
GO	98	60	9.5
GrO	90	87.5	2

As for the removal efficiency, GO and GrO showed positive results only for MB and MG dye types. MO adsorption is below 10%, hence was not taken into further analysis. MG adsorption on the other hand was 60% for GO and was not regular adsorption when refer to its time dependent graph. It decreased after 4-6 minutes and dropping after the 8 minutes. So further analysis was not possible due to this irregularity.

Adsorption Kinetics

To estimate the adsorption rate and mechanisms pseudo first and second order kinetics were used.

Pseudo 1st order: $\ln(q_e - q_t) = \ln q_{e,cal} - k_1 t$ (3)

K_1, the first order adsorption rate constant and $q_{e,cal}$, calculated equilibrium adsorption capacity was obtained by the intercept and slope of the graph $ln(q_e\text{-}q_t)$ vs. *t*.

Pseudo 2nd order: $\frac{t}{q_t} = \frac{1}{k_{obs} q_{e,cal}^2} + \frac{t}{q_{e,cal}}$ (4)

K_{obs} the second order adsorption rate constant and $q_{e,cal}$, calculated equilibrium adsorption capacity was obtained by the intercept and slope of the graph t/q_t vs. *t*. Table 2 shows the results obtained from the adsorption kinetics analysis.

Adsorption isotherms (A.I.)

Langmuir (LI) and Freundlich isotherms (FI) were used to understand the interface relationship between the adsorbate molecule and the adsorbent material at equilibrium. Hence, maximum adsorption capacity was determined by changing the initial dye concentration from 10 to 30 mg/L at room temperature (25 ^{0}C) with liquid/solid ratio of 5 L/g, pH of 5.5 and 300 rpm stirring speed. Langmuir isotherm was determined by Equation 5;

$$\frac{C_e}{q_e} = \frac{1}{K_L q_{max}} + \frac{C_e}{q_{max}} \quad (5)$$

Table 2: Comparison of Pseudo 1st and 2nd order model parameters

Model	Parameter	GO MB	GrO MB	GrO MG
Pseudo-1st order	$q_{e,\,cal}$ (mg/g)	0,691	1,537	0,756
	k_1 (g/mg.min)	0,499	0,481	0,297
	R^2	0,568	0,639	0,948
Psudo-2nd order	$q_{e,\,cal}$ (mg/g)	**8,264**	**4,348**	**3,802**
	k_2 (g/mg.min)	0,274	0,987	0,320
	R^2	0,998	0,999	0,999
Exp. value	q_e (mg/g)	**7,850**	**4,270**	**3,545**

Here, K_L, Langmuir rate constant and q_{max}, the maximum adsorption capacity would be determined by the graph C_e/q_e vs. *Ce*. Moreover, R_L correction factor for LI was determined using the following equation:

$$R_L = \frac{1}{1+K_L C_0} \quad (6)$$

FI was determined by:

$$\ln q_e = \ln K_F + \frac{1}{n} \ln C_e \quad (7)$$

FI rate constant, K_L (L/mg) and unit less correction factor ,*1/n* were determined by the graph *ln* q_e vs. C_e. Table 3 shows the results obtained for each isotherm parameter.

Table 3: Comparison of Langmuir and Feundlich isotherm parameters

Isotherm	Param:	GO+MB	GrO+MB	GrO+MG
Langmuir	q_{max} (mg/g)	62,893	202,429	113,122
	K_L (L/mg)	3,804	0,235	0,302
	R^2	0,999	0,829	0,974
	R_L	0,214	0,834	0,822
Freundlich	K_F (L/mg)	6,890	4,306	3,222
	1/n	-0,549	-0,148	-0,0711
	R^2	0,857	0,980	0,149

Adsorption kinetic results suggest that adsorption mechanism follows 2nd order adsorption (4), with higher R^2 value and similar equilibrium adsorption capacity. Adsorption isotherm results suggest that adsorption follows Langmuir model (5) with higher R^2 values and better R_L correction factors. Hence, we assume that adsorption takes place on a homogeneous surface with monolayer coverage and that no contact would occur later between adsorbate molecules.

4. Conclusion

Preparation of GO, GrO and EG was possible from the graphite recovered from spent LIB. This is mainly due to the increased interlayer distance between the graphitic layers in the structure due to the continues charge and discharge cycles. EG was not a good candidate for the adsorption of MB, MG and MO dye waste. Hence, trials should be carried out with other dye types or organic pollutants. However, GO performed really well absorbing MB and GrO performed well with both MB and MG. Corresponding maximum adsorption capacity based on Langmuir model for MB with GO is 62.89 mg/g and MB and MG with GrO is 202.43, 113.12 mg/g respectively. Accordingly, we can conclude that, for dye adsorption the best materials derive from the waste graphite from EoL LIBs is the Graphene Oxide. However, economic, and environmental sustainability of the production of the same from waste graphite should be evaluated further.

Acknowledgement: This research was Funded in part by a grant from the Italian Ministry of Foreign Affairs and International Cooperation and São Paulo Research Foundation. The authors would like to acknowledge the Fundação de Amparo à Pesquisa do Estado de São Paulo and Capes (grants: 2012/51871-9, 2019/11866-5, 2020/00493-0, 2021/14842-0 São Paulo Research Foundation).

References:

Dhakate, S. R., Chauhan, N., Sharma, S., Tawale, J., Singh, S., Sahare, P. D., & Mathur, R. B. (2011). An approach to produce single and double layer graphene from re-exfoliation of expanded graphite. *Carbon*, *49*(6), 1946–1954.

Guimarães, L. F., Botelho Junior, A. B., & Espinosa, D. C. R. (2022). Sulfuric acid leaching of metals from waste Li-ion batteries without using reducing agent. *Minerals Engineering*, *183*, 107597.

Hidayah, N. M. S., Liu, W. W., Lai, C. W., Noriman, N. Z., Khe, C. S., Hashim, U., & Lee, H. C. (2017). Comparison on graphite, graphene oxide and reduced graphene oxide: Synthesis and characterization. *AIP Conference Proceedings*, *1892*.

Lahiri, I., & Choi, W. (2013). Carbon Nanostructures in Lithium Ion Batteries: Past, Present, and Future. *Critical Reviews in Solid State and Materials Sciences*, *38*(2), 128–166.

Ma, X., Chen, M., Chen, B., Meng, Z., & Wang, Y. (2019). High-Performance Graphite Recovered from Spent

Lithium-Ion Batteries. *ACS Sustainable Chemistry and Engineering*, *7*(24), 19732–19738.

Maroufi, S., Assefi, M., Khayyam Nekouei, R., & Sahajwalla, V. (2020). Recovery of lithium and cobalt from waste lithium-ion batteries through a selective isolation-suspension approach. *Sustainable Materials and Technologies*, *23*, e00139.

Ogino, I., Yokoyama, Y., Iwamura, S., & R. Mukai, S. (2014). Exfoliation of Graphite Oxide in Water without Sonication: Bridging Length Scales from Nanosheets to Macroscopic Materials. *Chemistry of Materials*, *26*(10), 3334–3339.

Premathilake, D. S., Botelho Junior, A. B., Tenório, J. A. S., Espinosa, D. C. R., & Vaccari, M. (2023). Designing of a Decentralized Pretreatment Line for EOL-LIBs Based on Recent Literature of LIB Recycling for Black Mass. *Metals*, *13*(2), 374.

S. Hummers Jr., W., & E. Offeman, R. (2002). Preparation of Graphitic Oxide. *Journal of the American Chemical Society*, *80*(6), 1339–1339.

Saikam, L., Arthi, P., Jayram, N. D., & Sykam, N. (2022). Rapid removal of organic dyes from aqueous solutions using mesoporous exfoliated graphite. *Diamond and Related Materials*, *130*, 109480.

T. Tanabe, K. Niwase, N. Tsukuda, & E. Kuramoto. (1992). On the characterization of graphite. *Journal of Nuclear Materials*, *191*(194), 330–334.